Adsorption (2014) 20:631–647
DOI 10.1007/s10450-014-9608-x

Adsorption isotherms of CO_2, CO, N_2, CH_4, Ar and H_2 on activated carbon and zeolite LiX up to 1.0 MPa

Yongha Park · Dong-Kyu Moon · Yo-Han Kim · Hyungwoong Ahn · Chang-Ha Lee

Received: 17 December 2013 / Revised: 1 March 2014 / Accepted: 3 March 2014 / Published online: 22 March 2014

Abstract The adsorption isotherms of CO_2, CO, N_2, CH_4, Ar, and H_2 on activated carbon and zeolite LiX were measured using a volumetric method. Equilibrium experiments were conducted at 293, 308, and 323 K and pressures up to 1.0 MPa. The adsorption isotherm and heat of adsorption were analyzed for two pressure regions of experimental data: pressures up to 0.1 MPa and up to 1.0 MPa. Each experimental isotherm was correlated by the Langmuir, Sips, Toth and temperature dependent Sips isotherm models, and the deviation of each model was evaluated. The Sips and Toth models showed smaller deviation from the experimental data of adsorbents than the Langmuir model. Isosteric heats of adsorption were calculated by the temperature dependent Sips model and are presented along with surface loading. From deviation analysis, it is recommended that the isotherm in the proper pressure range be used to appropriately design adsorptive processes.

Keywords Activated carbon · Zeolite LiX · Adsorption isotherm · Syngas · Reforming gas

List of symbols

B	Langmuir, Sips, and Toth isotherm parameter (kPa^{-1})
DQ_{aver}	Adsorbed amount average deviation (%)
i	Isotherm data number (dimensionless)
K_1	1st parameters in the temperature dependence Sips model (mol kg^{-1})
K_2	2nd parameters in the temperature dependence Sips model (mol kg^{-1} K^{-1})
K_3	3rd parameters in the temperature dependence Sips model (kPa^{-1})
K_4	4th parameters in the temperature dependence Sips model (K)
K_5	5th parameters in the temperature dependence Sips model (dimensionless)
K_6	6th parameters in the temperature dependence Sips model (K)
k	Number of data (dimensionless)
n	Sips isotherm parameter (dimensionless)
P	Pressure (kPa)
Q_{st}	Isosteric heat of adsorption, (kJ mol^{-1})
q	Adsorbed amount moles, (mol kg^{-1})
q_m	Langmuir, Sips, and Toth isotherm parameter, (mol kg^{-1})
R	Ideal gas constant (J mol^{-1} K^{-1})
T	Temperature (K)
t	Toth isotherm parameter (dimensionless)

Y. Park · D.-K. Moon · Y.-H. Kim · C.-H. Lee (✉)
Department of Chemical and Biomolecular Engineering, Yonsei University, Seoul, Korea
e-mail: leech@yonsei.ac.kr

H. Ahn
Scottish Carbon Capture and Storage Centre, Institute for Materials and Processes, The University of Edinburgh, Edinburgh, UK

1 Introduction

Global warming caused by greenhouse gas (GHG) emissions has become one of the most important global issues. In addition, the need for hydrogen has greatly increased in various industrial fields where it is used as a chemical raw material or a clean fuel source.

Recently, many adsorption processes have been developed to capture CO_2 from emission gases. Increasing demand for hydrogen has provided strong economic motivation for the development of adsorption processes to

produce high purity H_2 from reforming gas, syngas, coke oven gas, and more traditional sources. Furthermore, the integrated gasification combined cycle (IGCC) generates massive amounts of hydrogen and carbon dioxide. The recovered H_2 may be supplied to H_2 turbines for green power generation as a next-generation IGCC process.

As a result, many kinds of adsorbents and adsorption technologies have been reported to resolve the issues of CO_2 capture and/or H_2 recovery from various effluent gases. The pressure swing adsorption (PSA) process is a promising process for such purpose from the gas streams (Chue et al. 1995; Gomes and Yee 2002; Yang and Lee 1998; Lee et al. 2008; Liu et al. 2011; You et al. 2012; Ahn et al. 2012; Schell et al. 2013).

In many studies, the capacity of newly developed adsorbents is compared with activated carbons and/or zeolites, which are widely applied in present industrial fields. Furthermore, since adsorption processes are based on preferential adsorption of desired gases onto a porous adsorbent at a certain pressure, adsorption equilibrium data of each component in a mixture are the most important factors in the design of adsorption processes. The effluent gases from power generators, coal gasifiers, coke combustors, reformers, and water–gas-shift reactors consist of a combination of CO_2, CO, N_2, CH_4, Ar and H_2 after undergoing various pretreatment processes such as particle removal, sour gas removal, sulfur removal/recovery, and/or drying.

To treat such effluent gases using adsorption processes, it is necessary to measure accurate single-component adsorption equilibrium data. In addition, since the adsorption processes can be operated at either low pressure or high pressure, adsorption isotherm data should be supplied in the proper pressure range to select appropriate adsorbents for design of efficient adsorption processes.

In this study, the adsorption isotherms of single components (CO_2, CO, N_2, CH_4, Ar and H_2) on activated carbon and zeolite LiX are presented. Adsorption isotherm data were measured at three temperatures of 293, 308, and 323 K and pressures up to 1.0 MPa. The experimental data were correlated with the Langmuir, Sips, Toth and temperature dependent Sips isotherm models. Fitting parameters and deviations were evaluated in ranges of low pressure ($\sim$ 0.1 MPa) and high pressure ($\sim$ 1.0 MPa). These results can contribute to the design of various adsorption processes for H_2 recovery and CO_2 capture. In addition, they can be used for the evaluation of adsorption capacity for newly developed adsorbents.

2 Experimental section

2.1 Material

Cylindrical activated carbon and spherical zeolite LiX were supplied by KURARAY CHEMICAL Co. (Coal-derived activated carbon; 2GA-H2J) and ZEOCHEM Co. (Z10-05-03), respectively. Prior to each experimental run, activated carbon was regenerated at 393 K in a vacuum oven, and zeolite LiX was regenerated at 623 K in an oven for longer than eight hours. BET analysis of the adsorbents was conducted with an automatic volumetric sorption analyzer (Quantachrome, ASIQM0V000-4) using nitrogen adsorption at 77 K. The measured and supplied physical properties of the adsorbents are detailed in Table 1. Gases used as adsorbates were of high purity (> 99.99 %).

Table 1 Physical properties of activated carbon and zeolite LiX

Property	Activated carbon	Zeolite LiX
Type	Cylindrical	Pellet
Particle size (mm)	1.7–2.36	1.5–1.7
Particle porosity (g/cm^3)	0.433	0.64
Average pore diameter (nm)	1.67	3.79[a]
Pellet density (g/cm^3)	0.85	2.4
Heat capacity (cal g^{-1} K^{-1})	0.25	0.42
Total surface area (m^2 g^{-1})	1,306.4	664.7

[a] Mesopore diameter of zeolite LiX pellet, not crystal pore size

2.2 Apparatus

Adsorption equilibrium was measured using a high pressure volumetric system (BELSORP-HP). Before the experimental run, about 0.5 g of the adsorbent was placed into the adsorption cell. In the method, the total amount of gas admitted into the system and the amount of gas in the vapor phase remaining after adsorption equilibrium were determined by appropriate P–V–T measurement.

2.3 Experimental procedure

After regeneration in a vacuum oven, the mass of the adsorbent was determined by a microbalance with an accuracy of $\pm$10 μg. Then, the samples were introduced into the adsorption cell after being purged by He twice. The measured adsorbents were put into the adsorption cell with a ceramic cap. To eliminate moisture and any trace of pollutants adsorbed during the installation of the adsorption cell, the activated carbon and zeolite LiX were reactivated at 393 and 623 K, respectively, under high vacuum for longer than 12 h. An oil diffusion pump and a mechanical vacuum pump maintained a vacuum on the system, and the evacuation was monitored with a pressure indicator.

The system, including gas storage tanks, lines, valves and gauges, was installed in an air bath, and the temperature of the internal system was kept constant by a temperature controller. Further, the temperature of the adsorption cell was controlled using a water bath circulator.

The temperature of the external connecting line between the system and adsorption cell was also controlled with an additional air bath temperature controller. The internal volume of the system and the dead volume in the adsorption system were determined by expansion of helium gas at the experimental temperature.

Before the experiment, the internal system was purged with helium gas and was evacuated with vacuum pumps. After purge/vacuum step three times, the desired amount of adsorptive gas was supplied to the internal system. During the experiment, all of the temperatures and pressures were recorded automatically on an interfaced computer. The amount of gas adsorbed was calculated from the measured temperature, pressure, and volume changes using compressibility factors obtained from NIST thermodynamic isotherm properties. (Linstrom and Mallard 2001)

3 Results and discussion

3.1 Adsorption isotherm

Because the excess adsorbed amounts were measured in the volumetric method (Sircar 1999), the excess adsorption isotherms of CO_2, CO, N_2, CH_4, Ar, and H_2 on activated carbon and zeolite LiX at 293, 308 and 323 K and pressures up to 1.0 MPa are compared in Figs. 1 and 2, respectively. And the isotherms of up to 0.1 MPa are simultaneously provided in the extended form of figures to clearly present the comparison with reference results at a low pressure range.

In the case of CO_2 on the activated carbon, the experimental data were compared with the published result at 323 K, as shown in Fig. 1a (Himeno et al. 2005; Kuro-Oka et al. 1984). Furthermore, the experimental adsorption isotherms of N_2 (Fig. 1c) and CH_4 (Fig. 1d) on the activated carbon were compared with the previous study performed at 293 and 323 K (Choi et al. 2003; Kuro-Oka et al. 1984). In the full pressure range of Figs. 1a, c, d, the average difference in the adsorbed amount of CO_2, N_2, and CH_4 between the results of this study and the reference results were 23, 17, and 9 %, respectively. Compared with the references in the full pressure range, their surface area and particle density of 1,150 $m^2\ g^{-1}$, 0.51 g/cm^3 (Coal-derived BPL, Calgon) and 1,150–1,250 $m^2\ g^{-1}$, 0.44 g/cm^3 (PCB, Calgon) were smaller than those of the activated carbon in the study (Choi et al. 2003; Himeno et al. 2005). In the low pressure range of Figs. 1a, d, the CO_2 and CH_4 isotherm showed 0.15 and 0.42 % difference at 323 K, respectively. Although the reference data came from the activated carbon fiber with a high surface area (KF-1500, Toyabo Co., Ltd.), the shapes of CO_2 and CH_4 isotherms in the two studies were similar to each other. The adsorption capacity of CO_2 on the activated carbon used was higher than the previous result while the activated carbon showed more favorable isotherm for CH_4 than the activated carbon reported in the reference.

The experimental results of CO_2, CO, N_2, CH_4, and Ar on zeolite LiX were also compared with the results of previous studies at 293 K, as shown in Figs. 2a–e (Park et al. 2006, 2008; Baksh et al. 1992). The average deviations in the adsorbed amount of each gas on zeolite LiX were 17, 31, 30, 37, and 13 %, respectively. Zeolite LiX showed a more favorable isotherm for CO_2 than the previous result, but the saturated amount was slightly lower. On the contrary, the adsorption isotherms of CO, N_2, CH_4 and Ar in the study were larger and more favorable than the previous results.

The surface area of zeolite LiX in the references was smaller by about 130 $m^2\ g^{-1}$ than that in the study. And the level of alkali metal ion exchange in zeolite LiX crystal can be different by using the applied ion exchange method (Pillai et al. 2010; Walton et al. 2006). As shown in Fig. 2c for N_2, a large difference among the studies was observed. And the adsorption isotherms of zeolite LiX pellets were smaller than zeolite LiX powder (Baksh et al. 1992). Therefore, it is expected that the amount of binder needed to make a pellet and ion exchange level may lead to the difference in the adsorption capacity between zeolite LiX pellets.

Considering the different total surface areas and shapes of the adsorbent manufactured by different companies, the experimental results were reasonable. Furthermore, the experimental reproducibility of both adsorbents was confirmed within 4 % for CO_2 by experiments repeated in triplicate and as less than 3 % for CO, CH_4, N_2 and Ar by experiments repeated in duplicate under the same conditions.

The isotherms of CO_2, CO, N_2, CH_4, and Ar isotherms on activated carbon and isotherms of CO_2, CO, N_2, and CH_4 isotherms on zeolite LiX up to 1.0 MPa showed convex curvature of Type I, as shown in Figs. 1a–e and 2a–d. However, the N_2 and Ar isotherms up to 0.1 MPa and H_2 isotherms up to 1.0 MPa on activated carbon were nearly linear. Isotherms of Ar and H_2 on zeolite LiX up to 1.0 MPa were also linear. The order of adsorption amount was $CO_2 \gg CH_4 > CO > N_2 \geq Ar \gg H_2$ for activated carbon and $CO_2 \gg CO > CH_4 \geq N_2 > Ar \gg H_2$ for zeolite LiX for isotherms in both the low pressure range ($\sim$0.1 MPa) and high pressure range ($\sim$1.0 MPa).

The adsorption amount of CO_2 on activated carbon at high pressure was greater than that of zeolite LiX, while the result in the low pressure region was opposite due to the strong adsorption affinity of CO_2 on zeolite LiX. The adsorption amount of CO on zeolite LiX was greater than that on activated carbon in both pressure ranges, showing

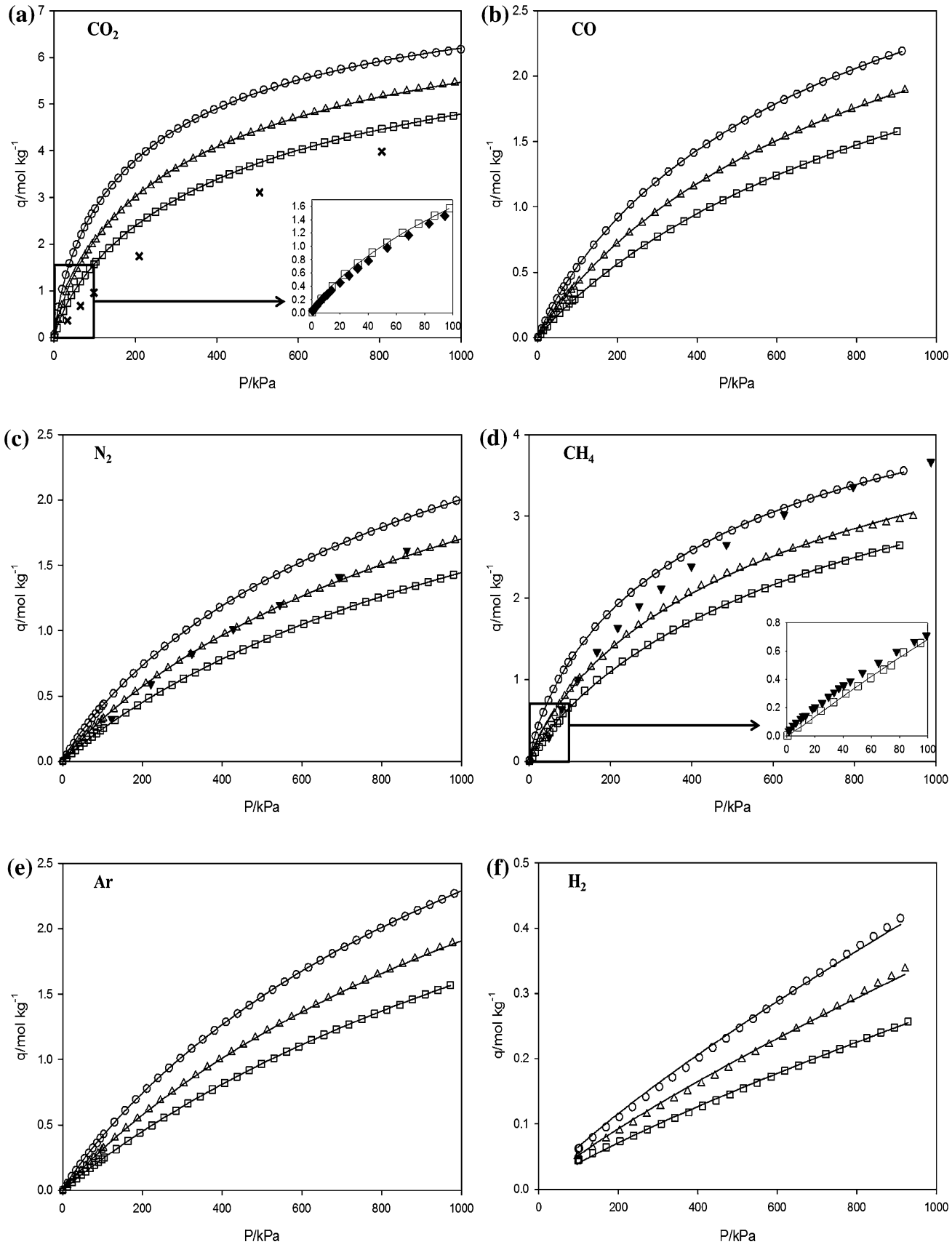
(a)
CO2
q/mol kg-1
P/kPa
(b)
CO
q/mol kg-1
P/kPa
(c)
N2
q/mol kg-1
P/kPa
(d)
CH4
q/mol kg-1
P/kPa
(e)
Ar
q/mol kg-1
P/kPa
(f)
H2
q/mol kg-1
P/kPa

◀**Fig. 1** Adsorption isotherms on activated carbon **a** CO_2, **b** CO, **c** N_2, **d** CH_4, **e** Ar, and **f** H_2 (*white circle*, T = 293 K; *white up pointing triangle*, T = 308 K; *white square*, T = 323 K; *black down pointing triangle*, T = 293 K, Choi et al. 2003; *times*, T = 323 K, (Himeno et al. 2005); *filled diamond*, T = 323 K (Kuro-Oka et al. 1984); *straight line*, Sips model)

much stronger adsorption affinity in the low pressure range, as illustrated in Figs. 1b and 2b. Further, the adsorption amount of N_2 on zeolite LiX was similar to that on activated carbon, but the adsorption affinity on zeolite LiX was much stronger than that on activated carbon, as shown at low pressure in Figs. 1c and 2c. On the other hand, the adsorption isotherms of CH_4 and Ar on activated carbon were higher than those on zeolite LiX for all pressure ranges.

Although there are large differences in surface area between the two adsorbents listed in Table 1, the results of CO_2, CO and N_2 on zeolite LiX were less affected by the surface area because the adsorption was more highly affected by the stronger attractive force between the adsorbate and adsorbent than between the molecules of the adsorbate in the bulk state. The effect of surface area on adsorption was clearly shown in H_2 isotherms, which have almost negligible adsorption affinity. The adsorption isotherm of H_2 on activated carbon at 293 K was almost twice as high as that on zeolite LiX, as shown in Figs. 1f and 2f, similar to the surface area difference ratio shown in Table 1.

3.2 Adsorption isotherm models

For each set of equilibrium data, rigorous assessments were performed and correlated using several pure-species equilibrium models. The isotherm equations used in this study were Langmuir, Toth, and Sips models (Do Duong 1998).

The Langmuir isotherm model is in general use for physical adsorption from gas or liquid solutions. This expression is based on a kinetic principle, that is, the rate of adsorption is equal to the rate of desorption from the surface:

$$q = \frac{q_m BP}{1 + BP}$$

where q is the number of adsorbed moles, P is equilibrium pressure, and q_m and B are Langmuir isotherm parameters.

Recognizing the problem of the continuing increase in the adsorbed amount with an increase in pressure or concentration in the Freundlich isotherm model, Sips proposed an equation similar in form to the Freundlich isotherm model but with a finite limit when the pressure is sufficiently high. The mathematical form of the isotherm model is

$$q = \frac{q_m (BP)^{1/n}}{1 + (BP)^{1/n}}$$

where q_m, B and n are isotherm parameters.

For a useful description of the adsorption equilibrium data at various temperatures, it is important to have the temperature dependent form of an isotherm model. The temperature dependence of Sips isotherm model for the affinity constant (B) may take the following form (Do Duong 1998).

$$B = K_3 \exp(K_4/T)$$

The temperature dependent form of the saturation capacity (q_m) and exponent (n) are empirical and the following form is chosen because of its simplicity.

$$q_m = K_1 + K_2 T$$

$$n = K_5 + K_6/T$$

The previous Sips isotherm model has limitations. Specifically, the Sips isotherm model is not valid at low pressure as it does not possess the correct low Henry-type behavior. The Toth isotherm model was introduced to address the above limitation. The Toth isotherm model is a semi-empirical expression that effectively describes many systems with sub-monolayer coverage. Because of its simplicity in form and its accurate behavior at low and high pressures, the Toth isotherm model is used in many applications for fitting data of many adsorbates on activated carbon as well as zeolites (Do Duong 1998; Myers and Belfort 1984; Lee et al. 2002). It is a three-parameter model usually written as:

$$q = \frac{q_m BP}{\left(1 + (BP)^t\right)^{1/t}}$$

where q_m, B, and t are numerically determined isotherm parameters.

Experimental data were divided into two pressure ranges for comparison of the fitting parameters and deviations: 0 to 0.1 MPa and 0 to 1.0 MPa. The fitting of Langmuir, Sips, Toth, and temperature dependent Sips isotherm models to the experimental data was performed with MATLAB 7.4 (Mathworks, Inc.) using a nonlinear curve-fitting procedure.

In this study, the experimental deviation from isotherm models was calculated using the following average percent deviation (DQ_{aver}) equations:

$$DQ_{aver}/\% = \frac{100}{k} \sum_{j=1}^{k} \left| \frac{q_j^{\exp} - q_j^{cal}}{q_j^{\exp}} \right|$$

where q^{exp} and q^{cal} are the experimental and calculated moles adsorbed, respectively, and k is the number of data points at a given temperature.

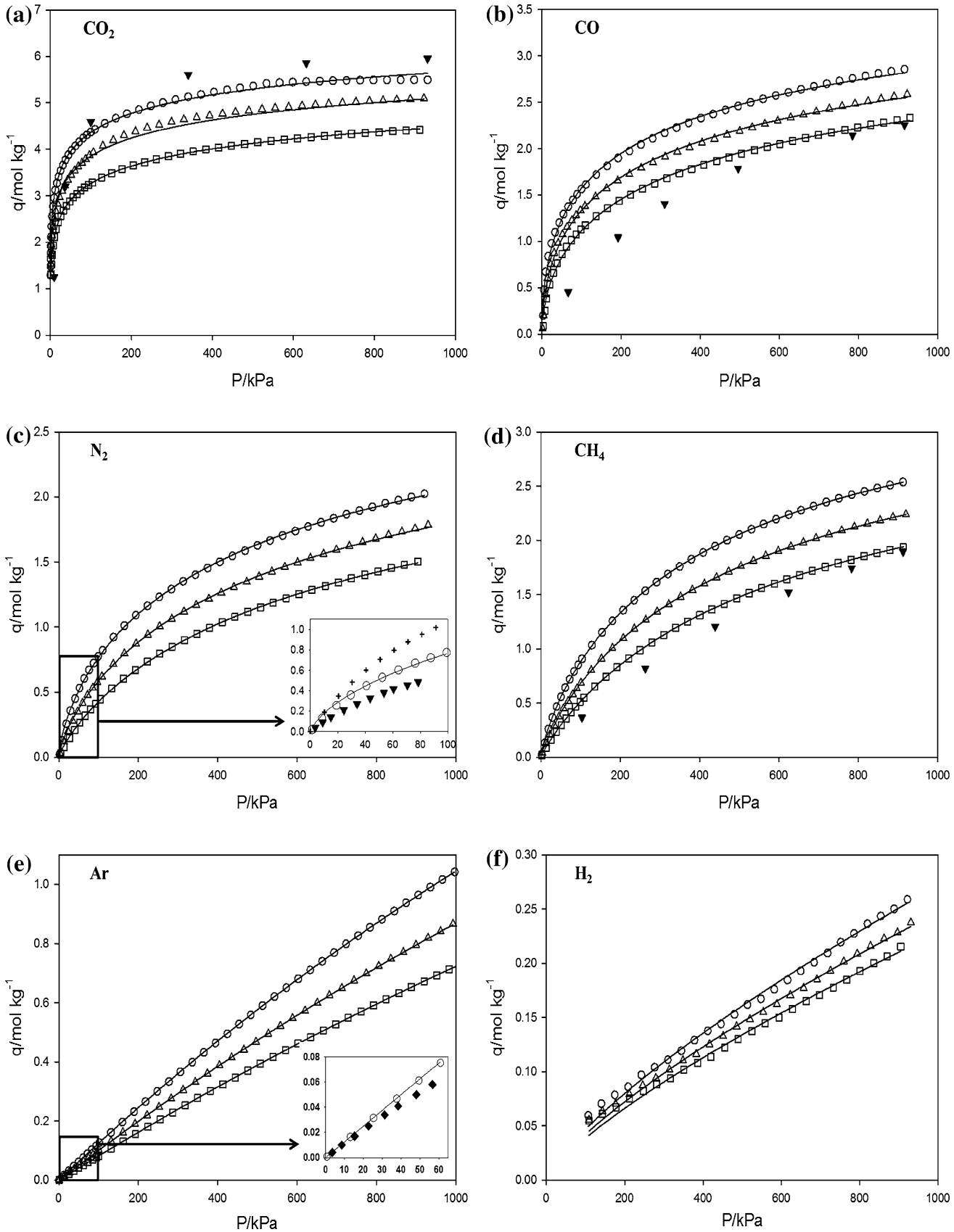
(a)
CO2
q/mol kg-1
P/kPa
(b)
CO
q/mol kg-1
P/kPa
(c)
N2
q/mol kg-1
P/kPa
(d)
CH4
q/mol kg-1
P/kPa
(e)
Ar
q/mol kg-1
P/kPa
(f)
H2
q/mol kg-1
P/kPa

◀**Fig. 2** Adsorption isotherms on zeolite LiX **a** CO_2, **b** CO, **c** N_2, **d** CH_4, **e** Ar, and **f** H_2 (*white circle*, T = 293 K; *white up pointing triangle*, T = 308 K; *white square*, T = 323 K; *black down pointing triangle*, T = 293 K (Park et al. 2008); *filled diamond*, T = 293 K (Park et al. 2006); *plus sign*, T = 293 K (Baksh et al. 1992); *straight line*, Sips model)

The isotherm parameters for these models are given in Tables 2, 3, 4, 5 and 6, respectively. As shown in Figs. 1 and 2, the isotherm models accurately predicted the experimental data. The Sips and Toth models provided better fits than the Langmuir model.

The fitting deviation (DQ_{aver}) at low pressure was lower than that at high pressure. Further, experimental equilibrium data with DQ_{aver} at high pressure (~1.0 MPa) and low pressure (~0.1 MPa) are presented in Tables 7, 8, 9, 10, 11 and 12 for activated carbon and Tables 13, 14, 15, 16, 17 and 18 for zeolite LiX. This result implies that the isotherm in the proper pressure range should be utilized to appropriately design adsorptive processes.

3.3 Isosteric heat of adsorption

Information related to heat release is important in an adsorption kinetic study and an adsorption bed dynamic study. The portion of heat adsorbed by the solid increases the particle temperature, and this increase in temperature affects the adsorption kinetics.(Do Duong 1998; Ahn et al. 2002, 2004) The isosteric heat of adsorption, Q_{st}, can be calculated from experimental isotherms at different temperatures, or it can be derived from any isotherm equation. And the heat of adsorption can be calculated by taking numerical derivatives from the isotherm model prediction at different temperatures (Talu and Kabel 1987). In this study, the isosteric heat of adsorption was calculated from the temperature dependence of the equilibrium capacity using the Clausius–Claypeyron equation (Do Duong 1998; Hill 1949; Nam et al. 2005; Suzuk 1990) along with the temperature dependent Sips isotherm model.

At two different temperatures with the same adsorbed amount or pressure, the isosteric heat of adsorption can be expressed directly. The data can be numerically integrated to determine the isosteric heat of adsorption by following the form of the Clausius–Claypeyron equation:

$$\frac{\Delta Q_{st}}{RT^2} = \left[\frac{\partial \ln P}{\partial T}\right]_q$$

$$\frac{\Delta Q_{st}}{RT^2} dT = d\ \ln P$$

$$\Delta Q_{st} = R\frac{\ln P_1/P_2}{(1/T_1) - (1/T_2)}$$

Table 2 Parameters of Langmuir model at pressure up to 0.1 MPa and 1.0 MPa

Gas	T (k)	Activated carbon				Zeolite LiX			
		~0.1 MPa		~1.0 MPa		~0.1 MPa		~1.0 MPa	
		q_m (mol kg^{-1})	B × 10^3 (1/kPa)	q_m (mol kg^{-1})	B × 10^3 (1/kPa)	q_m (mol kg^{-1})	B × 10^3 (1/kPa)	q_m (mol kg^{-1})	B × 10^3 (1/kPa)
CO_2	293	4.37	15.92	6.79	7.217	4.36	328.0	5.30	128.0
	308	3.83	11.43	6.36	4.933	3.72	315.0	4.76	99.50
	323	3.44	8.492	5.90	3.657	2.87	246.8	4.23	43.50
CO	293	2.37	3.008	3.53	1.700	1.77	58.07	2.88	13.40
	308	2.31	2.217	3.42	1.300	1.66	38.94	2.65	10.90
	323	1.97	1.907	3.21	1.100	1.55	26.33	2.47	8.500
N_2	293	2.29	2.300	3.45	1.350	1.55	10.11	2.43	4.370
	308	2.27	1.663	3.33	1.030	1.45	6.474	2.33	3.100
	323	2.24	1.247	3.18	0.821	1.44	4.265	2.18	2.290
CH_4	293	3.11	6.510	4.53	3.517	2.12	7.116	3.26	3.500
	308	3.04	4.010	4.28	2.414	2.14	4.641	3.12	2.600
	323	2.96	2.830	4.18	1.812	2.10	3.253	2.97	2.000
Ar	293	3.33	1.434	4.71	0.929	3.27	0.390	5.86	0.218
	308	3.25	1.074	4.55	0.721	3.07	0.337	5.80	0.177
	323	2.74	0.963	4.35	0.574	2.51	0.336	5.37	0.156
H_2				2.18	0.255			0.68	0.600
				1.80	0.246			0.64	0.670
				1.00	0.364			0.55	0.700

Table 3 Parameters of Sips model at pressure up to 0.1 MPa and 1.0 MPa

Gas	T (k)	Activated carbon						Zeolite LiX					
		~0.1 MPa			~1.0 MPa			~0.1 MPa			~1.0 MPa		
		q_m (mol kg^{-1})	$B \times 10^3$ (1/kPa)	*n*	q_m (mol kg^{-1})	$B \times 10^3$ (1/kPa)	*n*	q_m (mol kg^{-1})	$B \times 10^3$ (1/kPa)	*n*	q_m (mol kg^{-1})	$B \times 10^3$ (1/kPa)	*n*
CO_2	293	6.78	6.142	1.25	8.39	3.923	1.31	9.41	5.824	3.81	8.60	11.23	3.65
	308	6.05	4.570	1.20	8.10	2.566	1.29	8.67	4.403	3.70	8.00	7.712	3.55
	323	5.24	3.864	1.15	7.80	1.793	1.26	7.92	2.816	3.59	7.40	4.461	3.46
CO	293	2.67	2.501	1.02	4.20	1.201	1.11	2.38	25.10	1.48	4.65	2.595	2.02
	308	2.37	2.112	1.01	3.96	0.980	1.09	2.15	19.77	1.34	4.32	2.175	1.90
	323	2.07	1.821	0.99	3.73	0.795	1.07	1.91	15.86	1.20	3.99	1.868	1.77
N_2	293	4.05	1.053	1.06	4.29	0.863	1.11	1.80	7.473	1.09	3.48	1.696	1.41
	308	3.95	0.805	1.04	4.00	0.722	1.08	1.59	5.794	1.03	3.15	1.471	1.30
	323	3.86	0.635	1.03	3.71	0.621	1.06	1.37	4.640	0.98	2.82	1.272	1.20
CH_4	293	4.04	4.079	1.08	5.93	1.798	1.28	2.25	6.436	1.02	4.00	2.134	1.22
	308	3.88	2.980	0.99	5.73	1.234	1.22	2.17	4.551	1.00	3.71	1.770	1.16
	323	3.72	2.582	0.91	5.53	0.998	1.16	2.09	3.324	0.99	3.41	1.487	1.10
Ar	293	4.54	0.962	1.02	5.73	0.645	1.08	7.06	0.176	1.00	5.30	0.249	0.99
	308	4.34	0.742	1.02	5.32	0.542	1.05	6.70	0.163	0.98	5.02	0.213	0.99
	323	4.14	0.586	1.02	4.91	0.470	1.03	6.34	0.153	0.97	4.74	0.184	0.99
H_2					34.1	0.005	1.20				15.5	0.005	1.30
					33.6	0.004	1.20				15.2	0.005	1.30
					33.2	0.003	1.20				14.8	0.005	1.29

Table 4 Parameters of Toth model at pressure up to 0.1 MPa and 1.0 MPa

Gas	T (K)	Activated carbon						Zeolite LiX					
		~0.1 MPa			~1.0 MPa			~0.1 MPa			~1.0 MPa		
		q_m (mol kg^{-1})	$B \times 10^3$ (1/kPa)	t	q_m (mol kg^{-1})	$B \times 10^3$ (1/kPa)	t	q_m (mol kg^{-1})	$B \times 10^3$ (1/kPa)	t	q_m (mol kg^{-1})	$B \times 10^3$ (1/kPa)	t
CO_2	293	16.2	9.494	0.40	9.97	10.17	0.54	9.70	11,960	0.24	6.84	2,979	0.34
	308	12.3	5.885	0.46	9.44	5.784	0.57	5.46	11,590	0.30	6.53	3,142	0.31
	323	11.0	3.799	0.50	9.02	3.802	0.59	5.29	6,046	0.27	6.38	3,852	0.27
CO	293	5.12	1.516	0.69	5.12	1.510	0.69	5.71	351.9	0.26	15.5	1,532	0.16
	308	4.98	1.081	0.73	4.96	1.086	0.72	3.08	66.61	0.44	10.8	261.3	0.20
	323	4.48	0.860	0.75	4.48	0.849	0.77	2.73	32.00	0.51	8.41	67.91	0.24
N_2	293	23.3	0.260	0.48	5.60	1.028	0.67	2.28	8.283	0.71	5.02	6.361	0.43
	308	21.6	0.192	0.51	5.10	0.778	0.72	2.02	5.235	0.80	4.59	3.343	0.48
	323	20.5	0.145	0.54	4.61	0.624	0.77	1.02	5.726	1.30	3.83	2.048	0.57
CH_4	293	6.08	3.900	0.66	6.08	3.902	0.66	4.39	4.068	0.64	4.80	3.880	0.60
	308	5.57	2.380	0.72	5.57	2.379	0.72	3.87	2.833	0.72	4.25	2.604	0.69
	323	5.18	1.660	0.80	5.18	1.655	0.80	3.52	1.989	0.80	3.90	1.756	0.74
Ar	293	32.0	0.162	0.52	7.45	0.675	0.72	24.4	0.058	0.49	4.07	0.308	1.21
	308	31.6	0.116	0.55	6.68	0.537	0.77	20.4	0.056	0.50	3.81	0.266	1.21
	323	30.5	0.088	0.58	6.02	0.438	0.82	16.8	0.054	0.54	3.50	0.235	1.21
H_2					1,795	0.001	0.20				140	0.011	0.20
					1,580	0.001	0.19				134	0.010	0.20
					1,250	0.001	0.20				125	0.010	0.20

Table 5 Temperature dependent parameters of Sips model at pressure up to 0.1 MPa

Gas	~0.1 MPa					
	K_1 (mol kg^{-1})	$K_2 \times 10^3$ (mol kg^{-1} K^{-1})	$K_3 \times 10^6$ (kPa^{-1})	K_4 (K)	K_5	K_6 (K)
Activated carbon						
CO_2	21.88	−5.150	34.38	1,517	0.187	311.9
CO	8.469	−1.980	81.48	1,003	0.698	95.49
N_2	5.955	−0.650	4.447	1,601	0.787	78.85
CH_4	7.177	−1.070	25.50	1,481	−0.833	562.1
Ar	8.499	−1.350	4.850	1,550	0.980	12.61
Zeolite LiX						
CO_2	24.00	−4.980	2.579	2,270	1.444	693.5
CO	6.971	−1.567	183.4	1,440	−1.542	885.7
N_2	5.959	−1.420	43.21	1,510	−0.001	318.4
CH_4	3.789	−0.527	5.233	2,084	0.692	95.8
Ar	14.04	−2.383	37.63	452	0.613	114.1

Table 6 Temperature dependent parameters of Sips model at pressure up to 1.0 MPa

Gas	~1.0 MPa					
	K_1 (mol kg^{-1})	$K_2 \times 10^3$ (mol kg^{-1} K^{-1})	$K_3 \times 10^6$ (kPa^{-1})	K_4 (K)	K_5	K_6 (K)
Activated carbon						
CO_2	14.12	−19.57	0.789	2,494	0.764	160.8
CO	8.810	−15.73	16.24	1,261	0.587	154.5
N_2	9.947	−19.30	22.37	1,070	0.508	176.6
CH_4	9.849	−13.37	3.181	1,850	−0.033	384.6
Ar	13.74	−27.33	21.14	1,001	0.592	141.9
H_2	43.50	−32.00	0.020	1,650	1.158	12.61
Zeolite LiX						
CO_2	20.28	−39.87	0.759	2,820	1.552	614.9
CO	11.10	−22.00	72.10	1,050	−0.627	775.1
N_2	9.844	−21.73	76.19	910	−0.852	661.9
CH_4	9.806	−19.80	43.69	1,140	−0.039	368.9
Ar	10.76	−18.63	9.699	950	0.959	9.456
H_2	22.38	−233.3	1.362	396	1.183	34.72

where P is pressure, T is temperature, R is the gas constant, and Q_{st} is the isosteric heat of adsorption.

When the surfaces are energetically homogeneous and there is no interaction between the adsorbed molecules, the isosteric enthalpy of adsorption is independent of the amount adsorbed.(Hill 1949) However, if different levels of surface energy exist and the interactions between the adsorbed molecules cannot be neglected, the isosteric heat of adsorption varies with the surface coverage (Bae and Lee 2005).

Figure 3a, b shows the isosteric heats of adsorption for activated carbon and zeolite LiX. The figures with a high loading range were obtained from the temperature dependent Sips isotherm model fitted in the full experimental range (~1.0 MPa), while the extended figure of the low loading range used parameters fitted by the low pressure range (~0.1 MPa). Adsorption isotherms of H_2 on each adsorbent were not measured due to the low adsorption amount in the low pressure range (~0.1 MPa). Therefore, the isosteric heat of adsorption was calculated from the isotherm parameters of full pressure range.

The order of heat of adsorption was $CO_2 \gg CH_4 > CO \geq N_2 \geq Ar \gg H_2$ for activated carbon and $CO_2 \gg CO > N_2 > CH_4 > Ar \gg H_2$ for zeolite LiX for isotherms

Table 7 Experimental adsorption isotherm data for CO_2 on activated carbon

P (kPa) 293 K	q (mol kg^{-1})	P (kPa)	q (mol kg^{-1})	P (kPa) 308 K	q (mol kg^{-1})	P (kPa)	q (mol kg^{-1})	P (kPa) 323 K	q (mol kg^{-1})	P (kPa)	q (mol kg^{-1})
9.79	0.657	370	4.790	8.77	0.389	387	4.029	6.73	0.208	406	3.410
19.0	1.040	393	4.886	18.3	0.686	410	4.125	14.5	0.398	430	3.499
28.4	1.347	416	4.978	29.5	0.966	434	4.215	23.3	0.577	455	3.586
37.2	1.590	440	5.066	37.9	1.144	458	4.303	32.7	0.747	480	3.669
46.8	1.820	465	5.149	46.7	1.311	483	4.387	42.9	0.907	505	3.749
54.9	1.994	490	5.229	55.9	1.470	508	4.470	53.3	1.058	531	3.827
65.7	2.203	515	5.306	65.4	1.619	534	4.547	64.3	1.200	557	3.901
74.7	2.362	541	5.378	75.3	1.762	560	4.623	75.6	1.337	583	3.973
83.9	2.511	568	5.447	82.9	1.865	586	4.695	87.0	1.463	610	4.042
92.7	2.650	595	5.514	93.0	1.993	613	4.765	97.5	1.573	637	4.109
101	2.762	622	5.576	102	2.102	640	4.830	102	1.621	664	4.175
114	2.934	649	5.636	117	2.265	667	4.895	119	1.772	692	4.237
128	3.100	677	5.694	132	2.422	695	4.956	135	1.917	720	4.297
142	3.262	705	5.748	148	2.573	723	5.016	153	2.060	748	4.355
157	3.418	733	5.800	164	2.719	751	5.074	171	2.194	776	4.412
173	3.567	762	5.850	182	2.860	779	5.129	189	2.325	805	4.465
190	3.714	791	5.897	200	2.998	808	5.182	209	2.451	834	4.518
207	3.853	820	5.943	218	3.129	837	5.233	229	2.573	863	4.568
225	3.988	850	5.986	237	3.256	866	5.282	249	2.691	893	4.616
244	4.118	879	6.026	257	3.380	896	5.330	270	2.805	922	4.664
263	4.241	909	6.065	277	3.497	925	5.375	291	2.914	952	4.709
283	4.361	939	6.103	298	3.612	955	5.419	313	3.020	981	4.753
304	4.476	969	6.137	319	3.722	985	5.461	336	3.122	1,011	4.795
325	4.585	999	6.171	341	3.828	1,015	5.502	358	3.221		
DQ_{aver} (HP, LP) : 0.32, 0.46 %				DQ_{aver} (HP, LP) : 0.40, 0.23 %				DQ_{aver} (HP, LP) : 0.43, 0.29 %			

Table 8 Experimental adsorption isotherm data for CO on activated carbon

P (kPa) 293 K	q (mol kg^{-1})	P (kPa)	q (mol kg^{-1})	P (kPa) 308 K	q (mol kg^{-1})	P (kPa)	q (mol kg^{-1})	P (kPa) 323 K	q (mol kg^{-1})	P (kPa)	q (mol kg^{-1})
9.79	0.069	391	1.414	10.1	0.051	358	1.094	8.02	0.031	432	1.000
19.0	0.129	424	1.480	18.2	0.091	391	1.155	15.4	0.058	465	1.052
30.1	0.198	456	1.543	31.5	0.151	423	1.217	24.1	0.089	498	1.101
37.2	0.240	488	1.601	37.5	0.177	456	1.277	40.7	0.143	532	1.149
47.8	0.298	520	1.662	46.8	0.217	489	1.334	55.5	0.189	565	1.197
59.4	0.359	553	1.714	52.2	0.239	522	1.388	72.1	0.238	599	1.241
65.7	0.390	585	1.768	62.0	0.279	555	1.440	79.1	0.259	632	1.281
74.0	0.431	618	1.819	69.1	0.306	588	1.492	88.0	0.282	666	1.323
83.9	0.476	651	1.863	77.2	0.337	621	1.539	93.4	0.295	700	1.361
97.5	0.535	683	1.912	84.8	0.365	654	1.586	107	0.335	734	1.402
110	0.593	716	1.958	91.0	0.387	688	1.629	139	0.422	767	1.438
141	0.710	749	2.001	104	0.434	721	1.674	171	0.497	801	1.475
171	0.818	782	2.042	135	0.535	754	1.714	203	0.572	835	1.511
202	0.922	815	2.079	166	0.627	787	1.750	236	0.641	868	1.545
233	1.019	848	2.120	198	0.717	821	1.790	268	0.708	902	1.578
265	1.108	881	2.157	229	0.802	854	1.827	301	0.775		
296	1.192	914	2.193	262	0.880	888	1.859	334	0.832		
328	1.270			294	0.953	921	1.895	366	0.891		
DQ_{aver} (HP, LP) : 0.72, 0.22 %				DQ_{aver} (HP, LP) : 0.92, 0.13 %				DQ_{aver} (HP, LP) : 0.32, 1.76 %			

Table 9 Experimental adsorption isotherm data for N_2 on activated carbon

P (kPa) 293 K	q (mol kg^{-1})	P (kPa)	q (mol kg^{-1})	P (kPa) 308 K	q (mol kg^{-1})	P (kPa)	q (mol kg^{-1})	P (kPa) 323 K	q (mol kg^{-1})	P (kPa)	q (mol kg^{-1})
9.75	0.050	421	1.231	10.9	0.040	466	1.069	11.4	0.031	513	0.938
18.8	0.095	450	1.282	20.8	0.076	495	1.114	22.4	0.061	543	0.976
28.0	0.139	478	1.332	31.1	0.112	525	1.158	33.0	0.089	574	1.014
37.1	0.180	507	1.381	41.2	0.146	555	1.200	43.7	0.116	605	1.051
46.2	0.220	536	1.428	51.2	0.178	584	1.242	54.2	0.142	635	1.086
55.4	0.259	565	1.474	61.0	0.209	614	1.282	64.4	0.166	666	1.121
64.6	0.296	595	1.518	70.7	0.239	645	1.321	74.6	0.191	697	1.155
73.6	0.332	624	1.561	80.2	0.267	675	1.359	84.9	0.214	729	1.188
82.7	0.366	654	1.602	89.6	0.294	705	1.396	94.5	0.236	760	1.220
91.5	0.399	684	1.644	98.1	0.319	736	1.432	104	0.256	791	1.252
99.2	0.425	713	1.682	102	0.329	767	1.467	132	0.316	822	1.284
103	0.439	744	1.721	128	0.399	797	1.503	159	0.374	854	1.313
128	0.520	774	1.758	155	0.467	828	1.536	188	0.430	885	1.343
153	0.599	804	1.794	182	0.532	860	1.569	216	0.484	917	1.372
178	0.674	834	1.831	209	0.595	890	1.600	245	0.535	948	1.401
204	0.745	865	1.865	237	0.655	922	1.631	274	0.585	980	1.429
230	0.815	895	1.899	265	0.713	953	1.663	303	0.634	1,012	1.457
256	0.881	926	1.932	293	0.768	984	1.693	333	0.681		
283	0.945	956	1.964	321	0.823	1,016	1.723	362	0.727		
310	1.007	987	1.996	349	0.876			392	0.771		
337	1.066	1,018	2.026	378	0.927			422	0.813		
365	1.123			407	0.976			452	0.856		
DQ_{aver} (HP, LP) : 0.93, 0.79 %				DQ_{aver} (HP, LP) : 0.78, 0.58 %				DQ_{aver} (HP, LP) : 1.62, 0.42 %			

Table 10 Experimental adsorption isotherm data for CH_4 on activated carbon

P (kPa) 293 K	q (mol kg^{-1})	P (kPa)	q (mol kg^{-1})	P (kPa) 308 K	q (mol kg^{-1})	P (kPa)	q (mol kg^{-1})	P (kPa) 323 K	q (mol kg^{-1})	P (kPa)	q (mol kg^{-1})
8.31	0.189	435	2.673	8.13	0.095	392	2.063	7.91	0.060	386	1.691
15.0	0.311	467	2.753	17.2	0.193	423	2.148	15.6	0.116	418	1.771
22.4	0.433	499	2.827	25.8	0.278	454	2.224	24.2	0.177	450	1.844
34.4	0.600	531	2.901	34.7	0.361	486	2.301	33.2	0.240	482	1.920
46.8	0.749	562	2.971	43.1	0.436	518	2.370	42.1	0.300	515	1.989
59.3	0.883	595	3.032	53.0	0.519	550	2.435	50.5	0.354	547	2.056
71.9	1.004	627	3.097	61.5	0.589	583	2.497	59.6	0.411	580	2.118
84.7	1.116	659	3.156	74.5	0.699	615	2.550	68.8	0.468	613	2.183
95.7	1.211	692	3.217	87.3	0.799	648	2.605	74.2	0.499	646	2.240
106	1.291	724	3.272	99.6	0.885	680	2.658	83.0	0.592	679	2.297
134	1.476	757	3.324	110	0.956	713	2.709	95.0	0.658	712	2.351
162	1.647	790	3.374	124	1.019	746	2.754	107	0.721	745	2.405
191	1.798	822	3.427	152	1.156	779	2.801	137	0.864	778	2.458
220	1.940	855	3.468	180	1.279	812	2.844	167	0.993	811	2.507
250	2.067	888	3.513	209	1.421	845	2.885	197	1.115	844	2.554
280	2.187	921	3.558	238	1.546	878	2.924	228	1.224	877	2.601
311	2.298			269	1.664	911	2.961	259	1.328	911	2.646
341	2.398			299	1.773	944	2.999	291	1.425		
372	2.497			330	1.876			322	1.520		
DQ_{aver} (HP, LP) : 0.93, 3.88 %				DQ_{aver} (HP, LP) : 3.35, 1.14 %				DQ_{aver} (HP, LP) : 4.30, 3.88 %			

Table 11 Experimental adsorption isotherm data for Ar on activated carbon

P (kPa) 293 K	q (mol kg^{-1})	P (kPa)	q (mol kg^{-1})	P (kPa) 308 K	q (mol kg^{-1})	P (kPa)	q (mol kg^{-1})	P (kPa) 323 K	q (mol kg^{-1})	P (kPa)	q (mol kg^{-1})
11.9	0.056	439	1.352	12.0	0.042	453	1.112	12.4	0.032	468	0.917
22.8	0.106	468	1.415	23.5	0.080	483	1.168	24.3	0.062	499	0.965
33.7	0.154	497	1.476	34.9	0.117	513	1.223	35.8	0.091	530	1.010
44.3	0.199	527	1.534	46.1	0.153	544	1.273	47.0	0.119		1.060
55.1	0.244	556	1.593	57.0	0.187	574	1.325	58.2	0.145	561	1.100
65.4	0.285	586	1.650	67.7	0.220	605	1.374	69.0	0.171	624	1.150
75.7	0.325	616	1.704	78.3	0.252	635	1.421	79.4	0.195	655	1.190
85.6	0.362	646	1.758	88.7	0.282	666	1.470	89.9	0.219	687	1.230
94.7	0.399	676	1.810	98.2	0.311	697	1.516	99.7	0.239	719	1.270
103	0.430	707	1.860	103	0.323	728	1.561	105	0.250	750	1.310
129	0.520	737	1.912	131	0.401	759	1.605	134	0.314	782	1.350
156	0.611	767	1.958	159	0.475	790	1.649	164	0.377	814	1.380
183	0.696	798	2.006	188	0.550	821	1.690	194	0.439	846	1.420
211	0.777	828	2.052	216	0.619	852	1.731	224	0.497	877	1.460
239	0.858	859	2.095	245	0.688	883	1.773	254	0.555	909	1.500
267	0.935	890	2.141	274	0.754	915	1.814	284	0.610	941	1.530
295	1.011	921	2.184	304	0.818	946	1.854	314	0.666	973	1.570
323	1.084	951	2.226	333	0.879	978	1.892	345	0.719		
352	1.154	982	2.269	363	0.940	1,009	1.931	376	0.771		
380	1.222	1,013	2.308	393	0.999			406	0.821		
DQ_{aver} (HP, LP) : 0.63, 0.19 %				DQ_{aver} (HP, LP) : 0.70, 0.30 %				DQ_{aver} (HP, LP) : 0.30, 0.42 %			

Table 12 Experimental adsorption isotherm data for H_2 on activated carbon

P (kPa) 293 K	q (mol kg^{-1})	P (kPa)	q (mol kg^{-1})	P (kPa) 308 K	q (mol kg^{-1})	P (kPa)	q (mol kg^{-1})	P (kPa) 323 K	q (mol kg^{-1})	P (kPa)	q (mol kg^{-1})
99.3	0.062	505	0.247	96.9	0.051	511	0.199	97.8	0.044	515	0.155
102	0.063	538	0.261	100	0.051	545	0.210	101	0.045	549	0.163
135	0.079	572	0.276	134	0.065	579	0.222	135	0.055	584	0.172
169	0.095	606	0.290	169	0.077	613	0.234	169	0.064	619	0.182
202	0.111	640	0.304	203	0.090	648	0.246	204	0.073	653	0.189
235	0.126	673	0.319	237	0.102	682	0.257	238	0.082	687	0.199
269	0.142	707	0.332	271	0.115	716	0.269	273	0.092	722	0.207
302	0.157	741	0.347	305	0.127	750	0.280	307	0.1	756	0.215
336	0.171	774	0.360	340	0.139	785	0.291	342	0.109	791	0.223
370	0.186	808	0.374	374	0.150	819	0.303	377	0.118	825	0.232
403	0.202	842	0.387	408	0.162	853	0.315	411	0.128	860	0.241
437	0.217	876	0.401	442	0.174	887	0.326	446	0.136	894	0.248
471	0.231	909	0.415	477	0.186	921	0.338	480	0.145	929	0.257
DQ_{aver} (HP) : 2.71 %				DQ_{aver} (HP) : 2.26 %				DQ_{aver} (HP) : 2.02 %			

in both the low pressure range ($\sim$0.1 MPa) and high pressure range ($\sim$1.0 MPa). The isosteric heat of CO_2 on zeolite LiX was much higher than that on activated carbon, which implied a strong adsorption affinity between zeolite LiX and CO_2. In addition, the isosteric heats of CO and N_2 on zeolite LiX were also higher than those of activated carbon. On the

Table 13 Experimental adsorption isotherm data for CO_2 on zeolite LiX

P (kPa) 293 K	q (mol kg^{-1})	P (kPa)	q (mol kg^{-1})	P (kPa) 308 K	q (mol kg^{-1})	P (kPa)	q (mol kg^{-1})	P (kPa) 323 K	q (mol kg^{-1})	P (kPa)	q (mol kg^{-1})
0.46	1.058	218	5.068	1.04	1.745	330	4.639	2.05	1.269	384	3.990
0.65	1.317	248	5.130	1.99	1.949	361	4.686	3.67	1.462	415	4.035
0.96	1.574	278	5.180	3.55	2.145	393	4.728	6.12	1.642	447	4.076
1.53	1.827	309	5.226	5.87	2.330	425	4.765	9.55	1.810	479	4.115
2.54	2.077	340	5.264	8.97	2.504	457	4.802	13.9	1.965	512	4.151
4.05	2.317	372	5.296	12.8	2.669	490	4.834	19.1	2.110	544	4.183
6.12	2.550	404	5.327	17.4	2.824	522	4.863	25.2	2.244	577	4.213
8.74	2.775	436	5.354	22.7	2.967	555	4.891	31.9	2.367	610	4.240
11.9	2.990	468	5.376	28.7	3.103	588	4.915	39.4	2.482	643	4.266
15.6	3.196	501	5.397	35.4	3.229	621	4.939	47.4	2.587	677	4.290
19.9	3.390	533	5.416	42.7	3.344	654	4.961	56.0	2.683	710	4.312
24.9	3.573	566	5.432	50.7	3.449	688	4.981	65.1	2.772	744	4.334
30.6	3.746	599	5.445	59.2	3.544	721	5.002	74.5	2.852	777	4.353
37.1	3.905	632	5.456	68.4	3.630	754	5.018	84.3	2.925	811	4.372
44.4	4.050	665	5.466	77.9	3.707	788	5.036	93.7	3.004	845	4.391
52.4	4.180	698	5.473	87.0	3.790	821	5.053	103	3.078	879	4.409
61.3	4.299	731	5.481	96.3	3.867	855	5.066	126	3.232	912	4.424
70.7	4.404	764	5.485	106	3.935	889	5.079	151	3.367		
80.7	4.496	798	5.488	130	4.077	922	5.096	177	3.482		
90.0	4.568	831	5.492	155	4.197			204	3.584		
99.5	4.635	865	5.493	182	4.300			232	3.674		
110	4.695	898	5.494	210	4.386			261	3.753		
135	4.815	931	5.493	239	4.463			291	3.823		
161	4.915			268	4.529			321	3.884		
DQ_{aver} (HP, LP): 0.69, 0.01 %				DQ_{aver} (HP, LP): 1.65, 1.19 %				DQ_{aver} (HP, LP): 0.17, 0.01 %			

Table 14 Experimental adsorption isotherm data for CO on zeolite LiX

P (kPa) 293 K	q (mol kg^{-1})	P (kPa)	q (mol kg^{-1})	P (kPa) 308 K	q (mol kg^{-1})	P (kPa)	q (mol kg^{-1})	P (kPa) 323 K	q (mol kg^{-1})	P (kPa)	q (mol kg^{-1})
4.46	0.474	370	2.278	3.51	0.201	373	2.016	7.29	0.250	409	1.825
8.87	0.672	401	2.328	7.51	0.429	404	2.065	11.1	0.382	441	1.867
15.3	0.838	432	2.373	13.5	0.602	436	2.108	19.0	0.532	473	1.908
23.3	0.977	464	2.418	21.2	0.750	467	2.151	28.3	0.660	504	1.947
32.8	1.097	495	2.460	30.3	0.875	499	2.191	38.7	0.768	537	1.983
43.2	1.201	527	2.499	40.4	0.981	531	2.229	50.0	0.861	569	2.020
54.2	1.293	559	2.537	51.5	1.073	563	2.267	62.1	0.943	601	2.053
65.7	1.374	591	2.574	63.1	1.154	596	2.302	74.1	1.012	633	2.086
77.7	1.447	622	2.607	75.1	1.225	628	2.335	86.7	1.075	666	2.118
88.5	1.507	655	2.640	85.9	1.282	661	2.367	97.9	1.127	699	2.148
99.6	1.562	687	2.671	96.8	1.333	693	2.400	109	1.175	732	2.178
110	1.613	719	2.700	108	1.382	726	2.429	137	1.273	765	2.205
137	1.719	752	2.729	135	1.483	758	2.458	165	1.357	798	2.231
164	1.814	784	2.758	163	1.572	791	2.485	194	1.434	831	2.258
192	1.898	817	2.785	191	1.654	824	2.513	224	1.503	864	2.282
221	1.974	850	2.811	221	1.727	857	2.537	254	1.567	897	2.306
250	2.044	883	2.834	250	1.793	890	2.563	284	1.626	930	2.332
279	2.110	916	2.859	280	1.854	923	2.588	315	1.680		
309	2.168			311	1.912			346	1.732		
DQ_{aver} (HP, LP): 1.46, 1.88 %				DQ_{aver} (HP, LP) : 2.73, 3.06 %				DQ_{aver} (HP, LP): 2.02, 1.80 %			

Table 15 Experimental adsorption isotherm data for N_2 on zeolite LiX

P (kPa) 293 K	q (mol kg^{-1})	P (kPa)	q (mol kg^{-1})	P (kPa) 308 K	q (mol kg^{-1})	P (kPa)	q (mol kg^{-1})	P (kPa) 323 K	q (mol kg^{-1})	P (kPa)	q (mol kg^{-1})
8.34	0.129	406	1.502	12.9	0.119	441	1.307	13.7	0.078	476	1.116
18.9	0.256	437	1.546	23.2	0.199	473	1.348	26.7	0.148	508	1.152
29.4	0.358	469	1.586	35.1	0.279	505	1.388	40.0	0.210	540	1.187
40.7	0.450	500	1.627	47.4	0.352	537	1.426	53.3	0.267	573	1.220
52.2	0.531	532	1.665	59.9	0.417	569	1.463	66.8	0.320	605	1.253
63.9	0.604	564	1.703	72.5	0.477	602	1.497	80.4	0.369	638	1.285
76.1	0.670	596	1.738	85.2	0.532	634	1.531	92.8	0.410	671	1.316
87.5	0.723	628	1.772	97.0	0.579	667	1.563	105	0.446	704	1.344
99.0	0.775	660	1.804	109	0.622	699	1.594	134	0.528	738	1.374
110	0.822	692	1.836	137	0.716	732	1.624	163	0.603	771	1.401
137	0.923	725	1.866	165	0.797	765	1.653	193	0.672	804	1.426
165	1.010	757	1.895	194	0.874	798	1.681	223	0.734	837	1.454
194	1.092	790	1.923	224	0.940	831	1.708	254	0.795	871	1.478
223	1.163	822	1.952	254	1.005	864	1.734	285	0.849	904	1.504
253	1.231	855	1.974	284	1.063	897	1.758	316	0.899		
283	1.291	888	1.999	315	1.119	930	1.785	348	0.948		
313	1.351	921	2.025	346	1.169			379	0.993		
344	1.403			378	1.218			411	1.037		
DQ_{aver} (HP, LP): 1.51, 2.11 %				DQ_{aver} (HP, LP): 1.43, 0.48 %				DQ_{aver} (HP, LP) : 1.20, 0.45 %			

Table 16 Experimental adsorption isotherm data for CH_4 on zeolite LiX

P (kPa) 293 K	q (mol kg^{-1})	P (kPa)	q (mol kg^{-1})	P (kPa) 308 K	q (mol kg^{-1})	P (kPa)	q (mol kg^{-1})	P (kPa) 323 K	q (mol kg^{-1})	P (kPa)	q (mol kg^{-1})
9.57	0.130	379	1.825	13.1	0.126	412	1.603	13.2	0.086	431	1.363
19.0	0.259	409	1.887	22.6	0.206	443	1.658	25.8	0.162	462	1.415
29.0	0.367	439	1.946	33.9	0.293	473	1.712	38.6	0.233	494	1.465
39.5	0.466	469	2.001	45.6	0.374	504	1.763	51.3	0.298	525	1.513
50.2	0.556	500	2.053	57.2	0.448	536	1.812	63.9	0.358	557	1.559
61.3	0.641	531	2.102	69.0	0.517	567	1.858	76.6	0.416	589	1.601
72.5	0.719	562	2.150	80.4	0.581	598	1.903	87.5	0.466	620	1.642
83.6	0.790	593	2.195	90.8	0.634	630	1.943	98.5	0.511	652	1.681
93.7	0.850	624	2.237	101	0.686	662	1.982	109	0.552	684	1.718
104	0.906	656	2.277	127	0.802	694	2.020	136	0.653	717	1.756
129	1.033	687	2.315	153	0.909	726	2.055	164	0.744	750	1.790
154	1.151	719	2.352	180	1.007	758	2.091	192	0.831	782	1.822
180	1.257	751	2.387	208	1.098	790	2.124	221	0.912	815	1.855
208	1.356	783	2.420	236	1.185	823	2.156	250	0.987	847	1.885
235	1.447	815	2.451	264	1.266	855	2.185	279	1.058	880	1.914
263	1.534	848	2.482	293	1.341	888	2.213	309	1.126	913	1.941
292	1.614	880	2.510	322	1.412	920	2.241	339	1.191		
320	1.689	913	2.537	352	1.480			370	1.252		
DQ_{aver} (HP, LP) : 0.90, 0.90 %				DQ_{aver} (HP, LP) : 0.69, 0.55 %				DQ_{aver} (HP, LP) : 0.58, 0.49 %			

Table 17 Experimental adsorption isotherm data for Ar on zeolite LiX

P (kPa) 293 K	q (mol kg^{-1})	P (kPa)	q (mol kg^{-1})	P (kPa) 308 K	q (mol kg^{-1})	P (kPa)	q (mol kg^{-1})	P (kPa) 323 K	q (mol kg^{-1})	P (kPa)	q (mol kg^{-1})
13.2	0.017	454	0.527	13.7	0.014	466	0.441	13.3	0.011	476	0.370
25.4	0.032	484	0.559	26.4	0.027	497	0.467	25.6	0.021	507	0.394
37.7	0.047	513	0.590	38.7	0.039	527	0.495	37.8	0.032	539	0.416
49.5	0.061	543	0.620	50.9	0.051	558	0.521	49.9	0.041	571	0.439
60.9	0.075	573	0.651	62.8	0.063	589	0.547	61.8	0.051	603	0.462
72.4	0.089	603	0.680	74.6	0.075	620	0.573	73.2	0.061	634	0.484
83.3	0.103	633	0.711	85.9	0.086	651	0.599	84.8	0.070	666	0.506
93.4	0.115	663	0.740	96.2	0.097	682	0.625	95.3	0.078	698	0.527
102	0.126	693	0.769	101	0.102	713	0.650	100	0.081	729	0.549
131	0.161	723	0.798	131	0.132	744	0.675	131	0.107	761	0.570
160	0.196	754	0.826	162	0.161	775	0.699	162	0.132	793	0.591
189	0.231	784	0.855	192	0.190	806	0.724	193	0.156	825	0.612
218	0.265	814	0.882	222	0.219	837	0.748	225	0.180	856	0.632
248	0.299	845	0.910	252	0.248	868	0.772	256	0.205	888	0.652
277	0.333	875	0.938	283	0.276	899	0.795	287	0.229	920	0.672
306	0.366	905	0.964	313	0.304	930	0.819	319	0.253	952	0.692
336	0.399	936	0.990	344	0.332	962	0.842	350	0.277	984	0.713
365	0.432	966	1.016	374	0.360	993	0.866	381	0.301	1,015	0.732
395	0.463	997	1.042	404	0.388			413	0.324		
DQ_{aver} (HP, LP) : 0.32, 0.19 %				DQ_{aver} (HP, LP) : 0.25, 0.70 %				DQ_{aver} (HP, LP) : 0.46, 2.36 %			

Table 18 Experimental adsorption isotherm data for H_2 on zeolite LiX

P (kPa) 293 K	q (mol kg^{-1})	P (kPa)	q (mol kg^{-1})	P (kPa) 308 K	q (mol kg^{-1})	P (kPa)	q (mol kg^{-1})	P (kPa) 323 K	q (mol kg^{-1})	P (kPa)	q (mol kg^{-1})
107	0.060	548	0.167	109	0.056	554	0.155	109	0.055	559	0.145
141	0.070	582	0.176	143	0.064	589	0.162	143	0.061	594	0.150
175	0.079	616	0.185	177	0.070	623	0.171	178	0.067	628	0.158
209	0.086	650	0.193	212	0.079	657	0.177	213	0.075	663	0.165
242	0.097	684	0.201	246	0.087	691	0.185	247	0.082	698	0.171
276	0.104	718	0.209	280	0.094	725	0.193	282	0.088	732	0.177
310	0.111	752	0.219	314	0.102	759	0.202	316	0.094	767	0.185
344	0.119	786	0.227	348	0.110	794	0.209	351	0.102	801	0.193
378	0.129	820	0.236	383	0.116	828	0.216	386	0.108	836	0.200
412	0.138	854	0.244	417	0.125	862	0.223	420	0.113	870	0.207
446	0.144	888	0.250	451	0.133	896	0.228	455	0.122	905	0.215
480	0.153	922	0.259	485	0.142	931	0.238	490	0.130		
514	0.162			520	0.148			524	0.137		
DQ_{aver} (HP) : 2.95 %				DQ_{aver} (HP) : 2.56 %				DQ_{aver} (HP) : 3.67 %			

other hand, in the case of CH_4 and Ar, activated carbon showed a higher isosteric heat of adsorption at a certain level compared to that of zeolite LiX.

The adsorption of all the molecules implied a vertical interaction stemming from the energetic heterogeneity of the surface. On the other hand, CO_2 on zeolite LiX showed

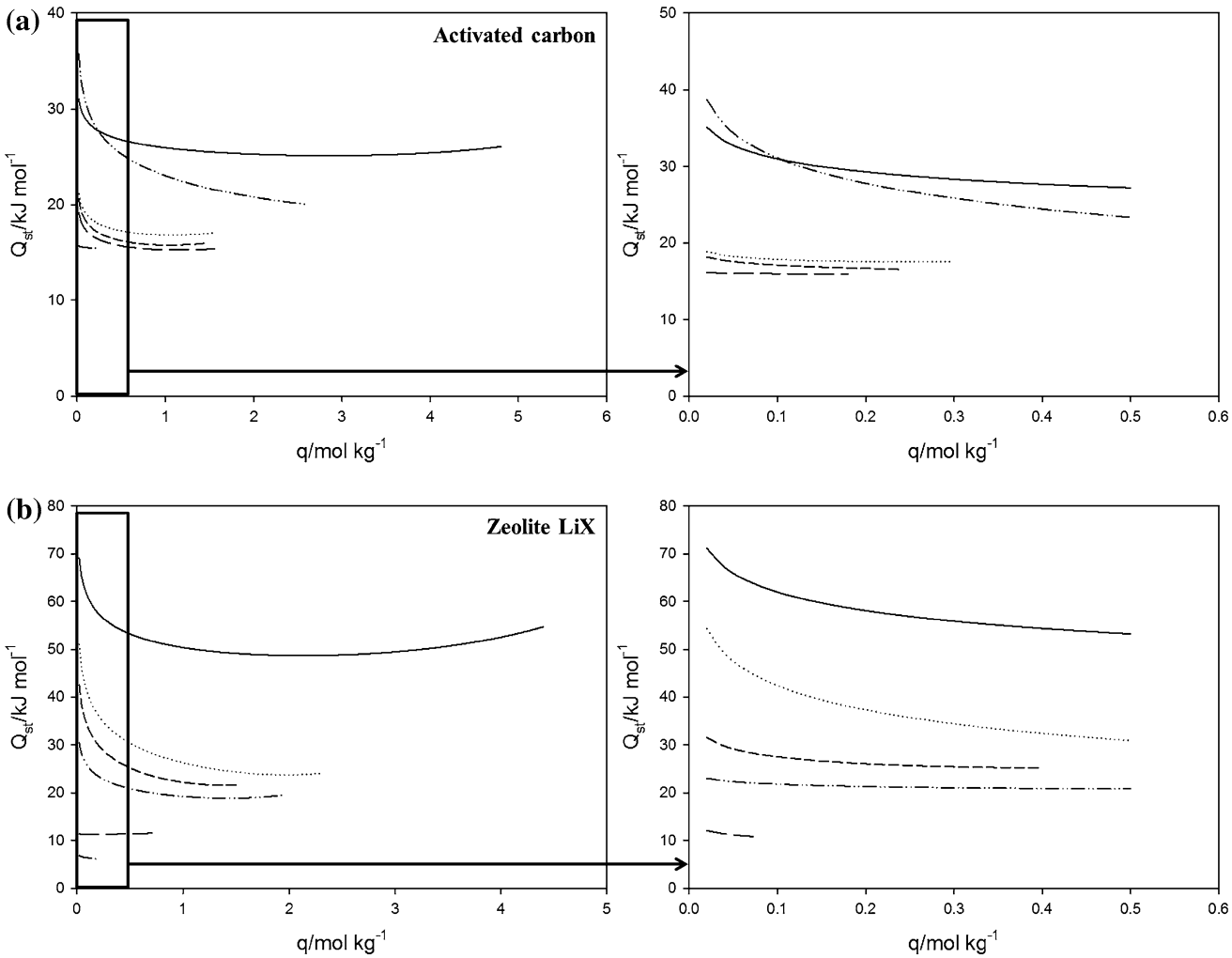

Fig. 3 Isosteric heat of adsorption on adsorbents with respect to surface loading **a** activated carbon and **b** Zeolite LiX (*straight line*, CO_2; *horizontal ellipses*, CO; *spaced hyphen lines*, N_2; *spaced n-dash lines with double dots*, CH_4; *spaced n-dash lines*, Ar; *spaced n-dash lines with single dot*, H_2)

lateral interactions between adsorbate molecules, resulting in an increase in adsorbed amount after about 3 mol/kg.

Except for Ar and H_2 on zeolite LiX, the adsorption of all the molecules implied a vertical interaction stemming from the energetic heterogeneity of the surface. On the other hand, CO_2 on activated carbon and CO_2 and CO on zeolite LiX showed lateral interactions between adsorbate molecules, resulting in an increase in adsorbed amount.

4 Conclusion

The adsorption isotherms of CO_2, CO, N_2, CH_4, Ar, and H_2 on activated carbon and zeolite LiX were measured at 293, 308, and 323 K and pressures up to 1.0 MPa. The order of adsorption amount was $CO_2 \gg CH_4 > CO > N_2 \geq Ar \gg H_2$ for activated carbon and $CO_2 \gg CO > CH_4 \geq N_2 > Ar \gg H_2$ for zeolite LiX. The saturated amount of CO_2 on activated carbon was higher than that on zeolite LiX. However, the adsorbed amounts on zeolite LiX in the low pressure range ($\sim$0.1 MPa) were larger than those on activated carbon due to the high adsorption affinity of zeolite LiX. From deviation analysis, it is recommended that the isotherm in the proper pressure range should be utilized to appropriately design adsorption processes.

Experimental data were correlated by the Langmuir, Sips, and Toth models. The Sips and Toth models showed small deviations from experimental data compared to the result from the Langmuir model. The order of heat of adsorption was $CO_2 \gg CH_4 > CO \geq N_2 \geq Ar \gg H_2$ for activated carbon and $CO_2 \gg CO > N_2 > CH_4 > Ar \gg H_2$ for zeolite LiX. The isosteric heat of CO_2 on zeolite LiX was much higher than that on activated carbon.

Further, zeolite LiX also showed higher isosteric heats of CO and N_2 than activated carbon.

These results can be used to accurately design adsorption processes by applying the isotherm data within the operating condition range.

Acknowledgments This work was supported by POSCO (2013 × 037), the Korea Institute of Energy Technology Evaluation and Planning (KETEP: 20118510020030-12-1-000) and the Ministry of Trade, Industry & Energy (MOTIE).

References

Ahn, H., Moon, J.-H., Hyun, S.-H., Lee, C.-H.: Diffusion mechanism of carbon dioxide in zeolite 4A and CaX pellets. Adsorption **10**(2), 111–128 (2004)

Ahn, H., Yoo, H.-K., Shul, Y., Hyun, S., Lee, C.-H.: Diffusion mechanism of N_2 and CH_4 in pelletized zeolite 4A, 5A and CaX. J. Chem. Eng. Jpn. **35**(4), 334–345 (2002)

Ahn, S., You, Y.-W., Lee, D.-G., Kim, K.-H., Oh, M., Lee, C.-H.: Layered two- and four-bed PSA processes for H_2 recovery from coal gas. Chem. Eng. Sci. **68**(1), 413–423 (2012). doi:10.1016/j.ces.2011.09.053

Bae, Y.-S., Lee, C.-H.: Sorption kinetics of eight gases on a carbon molecular sieve at elevated pressure. Carbon **43**(1), 95–107 (2005)

Baksh, M., Kikkinides, E., Yang, R.: Lithium type X zeolite as a superior sorbent for air separation. Sep. Sci. Technol. **27**(3), 277–294 (1992)

Choi, B.-U., Choi, D.-K., Lee, Y.-W., Lee, B.-K., Kim, S.-H.: Adsorption equilibria of methane, ethane, ethylene, nitrogen, and hydrogen onto activated carbon. J. Chem. Eng. Data **48**(3), 603–607 (2003)

Chue, K., Kim, J., Yoo, Y., Cho, S., Yang, R.: Comparison of activated carbon and zeolite 13X for CO_2 recovery from flue gas by pressure swing adsorption. Ind. Eng. Chem. Res. **34**(2), 591–598 (1995)

Do Duong, D.: Absorption Analysis: Equilibria and Kinetics, vol. 2. Imperial College, London (1998)

Gomes, V.G., Yee, K.W.: Pressure swing adsorption for carbon dioxide sequestration from exhaust gases. Sep. Purif. Technol. **28**(2), 161–171 (2002)

Hill, T.L.: Statistical mechanics of adsorption. V. Thermodynamics and heat of adsorption. J. Chem. Phys. **17**, 520 (1949)

Himeno, S., Komatsu, T., Fujita, S.: High-pressure adsorption equilibria of methane and carbon dioxide on several activated carbons. J. Chem. Eng. Data **50**(2), 369–376 (2005)

Kuro-Oka, M., Suzuki, T., Nitta, T., Katayama, T.: Adsorption isotherms of hydrocarbons and carbon dioxide on activated fiber carbon. J. Chem. Eng. Jpn. **17**(6), 588–592 (1984)

Lee, J.-S., Kim, J.-H., Kim, J.-T., Suh, J.-K., Lee, J.-M., Lee, C.-H.: Adsorption equilibria of CO_2 on zeolite 13X and zeolite X/activated carbon composite. J. Chem. Eng. Data **47**(5), 1237–1242 (2002)

Lee, J.J., Kim, M.K., Lee, D.G., Ahn, H., Kim, M.J., Lee, C.H.: Heat-exchange pressure swing adsorption process for hydrogen separation. AlChE J. **54**(8), 2054–2064 (2008)

Linstrom, P.J., Mallard, W.G.: NIST Chemistry WebBook; NIST Standard Reference Database No. 69. NIST, New York (2001)

Liu, Z., Grande, C.A., Li, P., Yu, J., Rodrigues, A.E.: Multi-bed Vacuum Pressure Swing Adsorption for carbon dioxide capture from flue gas. Sep. Purif. Technol. **81**(3), 307–317 (2011). doi:10.1016/j.seppur.2011.07.037

Myers, A.L., Belfort, G.: Fundamentals of adsorption. In. Engineering Foundation, New York (1984)

Nam, G.-M., Jeong, B.-M., Kang, S.-H., Lee, B.-K., Choi, D.-K.: Equilibrium isotherms of CH_4, C_2H_6, C_2H_4, N_2, and H_2 on zeolite 5A using a static volumetric method. J. Chem. Eng. Data **50**(1), 72–76 (2005)

Park, J.-Y., Yang, S.-I., Choi, D.-Y., Jang, S.-C., Lee, C.-H., Choi, D.-K.: Pure and binary gases adsorption equilibria of CO_2/CO/CH_4/H_2 on Li–X zeolite. Korean. Chem. Eng. Res. **46**(1), 175–183 (2008)

Park, Y.-J., Lee, S.-J., Moon, J.-H., Choi, D.-K., Lee, C.-H.: Adsorption equilibria of O_2, N_2, and Ar on carbon molecular sieve and zeolites 10X, 13X, and LiX. J. Chem. Eng. Data **51**(3), 1001–1008 (2006)

Pillai, R.S., Sethia, G., Jasra, R.V.: Sorption of CO, CH_4, and N_2 in alkali metal ion exchanged zeolite-X: grand canonical monte carlo simulation and volumetric measurements. Ind. Eng. Chem. Res. **49**(12), 5816–5825 (2010)

Schell, J., Casas, N., Marx, D., Blom, R., Mazzotti, M.: Comparison of commercial and new adsorbent materials for pre-combustion CO_2 capture by pressure swing adsorption. Energy Procedia **37**, 167–174 (2013). doi:10.1016/j.egypro.2013.05.098

Sircar, S.: Gibbsian surface excess for gas adsorption revisited. Ind. Eng. Chem. Res. **38**(10), 3670–3682 (1999)

Suzuk, M.: Adsorption engineering, vol. 551, pp. 128–132. Kodansha, Tokyo (1990)

Talu, O., Kabel, R.: Isosteric heat of adsorption and the vacancy solution model. AlChE J. **33**(3), 510–514 (1987)

Walton, K.S., Abney, M.B., Douglas LeVan, M.: CO_2 adsorption in Y and X zeolites modified by alkali metal cation exchange. Microporous Mesoporous Mater. **91**(1), 78–84 (2006)

Yang, J., Lee, C.H.: Adsorption dynamics of a layered bed PSA for H_2 recovery from coke oven gas. AlChE J. **44**(6), 1325–1334 (1998)

You, Y.-W., Lee, D.-G., Yoon, K.-Y., Moon, D.-K., Kim, S.M., Lee, C.-H.: H_2 PSA purifier for CO removal from hydrogen mixtures. Int. J. Hydrog Energy **37**(23), 18175–18186 (2012). doi:10.1016/j.ijhydene.2012.09.044